Received: 13 February 2023 | Revised: 24 August 2023 | Accepted: 27 August 2023

DOI: 10.1111/mmi.15151

RESEARCH ARTICLE

WILEY

Simvastatin induces human gut bacterial cell surface genes

Veronica Escalante[1] | Renuka R. Nayak[2,3] | Cecilia Noecker[1] | Joel Babdor[1,4] | Matthew Spitzer[1,4] | Adam M. Deutschbauer[5,6] | Peter J. Turnbaugh[1,7]

[1]Department of Microbiology & Immunology, University of California, San Francisco, California, USA

[2]Department of Medicine, San Francisco Veterans Affairs, San Francisco, California, USA

[3]Department of Medicine, University of California, San Francisco, San Francisco, California, USA

[4]Department of Otolaryngology-Head and Neck Surgery, University of California, San Francisco, San Francisco, California, USA

[5]Environmental Genomics and Systems Biology Division, Lawrence Berkeley National Laboratory, Berkeley, California, USA

[6]Department of Plant and Microbial Biology, University of California, Berkeley, Berkeley, California, USA

[7]Chan Zuckerberg Biohub-San Francisco, San Francisco, California, USA

Correspondence
Peter J. Turnbaugh, Department of Microbiology & Immunology, University of California, San Francisco, CA 94143, USA.
Email: peter.turnbaugh@ucsf.edu

Funding information
Burroughs Wellcome Fund, Grant/Award Number: 1017921; Chan Zuckerberg Biohub-San Francisco, Grant/Award Number: 7028823; National Center for Complementary and Integrative Health, Grant/Award Number: R01AT011117; National Heart, Lung, and Blood Institute, Grant/Award Number: R01HL122593; National Institute of Arthritis and Musculoskeletal and Skin Diseases, Grant/Award Number: R01AR074500; National Institute of Diabetes and Digestive and Kidney Diseases, Grant/Award Number: R01DK114034; National Institute of General Medical Sciences, Grant/Award Number: F32GM140808, R25GM056847 and RM1GM135102; National Science Foundation, Grant/Award Number: 1650113

Abstract

Drugs intended to target mammalian cells can have broad off-target effects on the human gut microbiota with potential downstream consequences for drug efficacy and side effect profiles. Yet, despite a rich literature on antibiotic resistance, we still know very little about the mechanisms through which commensal bacteria evade non-antibiotic drugs. Here, we focus on statins, one of the most prescribed drug types in the world and an essential tool in the prevention and treatment of high circulating cholesterol levels. Prior work in humans, mice, and cell culture support an off-target effect of statins on human gut bacteria; however, the genetic determinants of statin sensitivity remain unknown. We confirmed that simvastatin inhibits the growth of diverse human gut bacterial strains grown in communities and in pure cultures. Drug sensitivity varied between phyla and was dose-dependent. We selected two representative simvastatin-sensitive species for more in-depth analysis: *Eggerthella lenta* (phylum: Actinobacteriota) and *Bacteroides thetaiotaomicron* (phylum: Bacteroidota). Transcriptomics revealed that both bacterial species upregulate genes in response to simvastatin that alter the cell membrane, including fatty acid biogenesis (*E. lenta*) and drug efflux systems (*B. thetaiotaomicron*). Transposon mutagenesis identified a key efflux system in *B. thetaiotaomicron* that enables growth in the presence of statins. Taken together, these results emphasize the importance of the bacterial cell membrane in countering the off-target effects of host-targeted drugs. Continued mechanistic dissection of the various mechanisms through which the human gut microbiota evades drugs will be essential to understand and predict the effects of drug administration in human cohorts and the potential downstream consequences for health and disease.

KEYWORDS
antimicrobial resistance, bacterial genetics, drug efflux, human gut microbiome, transcriptomics

1 | INTRODUCTION

Population-level surveys of the human gut microbiota have revealed that pharmaceuticals are the top predictor of inter-individual variations in gut microbial community structure (Falony et al., 2016; Zhernakova et al., 2016. Surprisingly, this association extends beyond drugs for infectious disease to drugs used in a wide range of noncommunicable diseases, including cancer (Spanogiannopoulos et al., 2022), rheumatoid arthritis (Nayak et al., 2021), and cardiovascular disease (Falony et al., 2016; Vieira-Silva et al., 2020. The off-target of statins on the gut microbiota is of particular interest due to the ubiquity of the use of these drugs in patients and the existence of rare but potentially severe adverse effects, including muscle damage and diabetes (Golomb & Evans, 2008).

Studies in humans, mice, and cell culture support a robust and clinically relevant interaction between statins and the gut microbiota. Early work in humans demonstrated that bile acid metabolites produced by the gut microbiome are positively associated with statin bioavailability and efficacy (Kaddurah-Daouk et al., 2011), consistent with a recent metagenomic sequencing study demonstrating that the gut microbiome is associated with both statin efficacy and toxicity (Wilmanski et al., 2022). Statins may also have a broader beneficial effect on the gut microbiota, for example, by decreasing the risk of obesity (Vieira-Silva et al., 2020). While gold-standard data from double-blinded longitudinal randomized controlled trials remain lacking, experiments in mouse models support a direct causal effect of statins on the gut microbiota (Caparrós-Martín et al., 2017; Catry et al., 2015; Cheng et al., 2021; Xu et al., 2022; Zhang et al., 2021) and even a potential role of the gut microbiota in contributing to their lipid-lowering effects (He et al., 2017). Furthermore, a screen of human gut bacterial isolates suggested that statins can directly inhibit the growth of gut bacteria (Maier et al., 2018).

However, despite the extensive literature supporting an important interaction between statins and the gut microbiome, multiple key questions remain. The bacterial targets of statins remains a mystery, given that their canonical target, 3-hydroxy-3-methylglutaryl coenzyme A (HMG-CoA) reductase, is rarely found in the human gut microbiome (Gill et al., 2006). The one prior *in vitro* study (Maier et al., 2018) only evaluated a single dose of statins in mono-culture; thus, the minimal inhibitory concentration (MIC) and relevance of the observed growth inhibition to microbial communities remain unclear. Furthermore, although growth inhibition is a valuable starting point, far more work is needed to assess the impact of statins on bacterial physiology, gene expression, and metabolic activity. And perhaps most importantly, prior to this study we lacked any insight into the genes and gene products that contribute to bacterial sensitivity to statins or if these mechanisms were shared across phyla.

To address these major knowledge gaps, we conducted an in-depth analysis of the interactions of a single representative statin (simvastatin) and the human gut microbiota. Simvastatin was selected due to its clinical relevance and clear evidence for microbiota interactions in humans (Kaddurah-Daouk et al., 2011), mice (He et al., 2017; Xu et al., 2022), and cell culture (Maier et al., 2018). As expected, we found that simvastatin has dose-dependent effects on bacterial growth across phyla. Further, we used a combination of transcriptomics and transposon mutagenesis to identify pathways in representative strains from two bacterial phyla (one Gram-positive and one Gram-negative) that support bacterial growth in the presence of statins. These results emphasize the parallels between pathways for resistance to antibiotics and host-targeted drugs (Maier et al., 2018) while providing an experimental and conceptual framework to dissect the impact of a broader range of statins or other drugs on human gut bacteria.

2 | MATERIALS AND METHODS

2.1 | Media, strains, drugs used

BHI^{CHAV}: Bacto Brain Heart Infusion (BD Biosciences, 37 g/L) supplemented with L-cysteine-HCl (0.05%, w/v), hemin (5 μg/mL), L-arginine (1.0%, w/v), and vitamin K (1 μg/mL). BHI^{CHV}: Bacto Brain Heart Infusion (BD Biosciences, 37 g/L) supplemented with L-cysteine-HCl (0.05%, w/v), hemin (5 μg/mL), and vitamin K (1 μg/mL). Simvastatin: Toronto chemicals S485000. DMSO (anhydrous, ≥99.9%): Sigma-Aldrich Sure/Seal 276855. MeOH (anhydrous, ≥99.9%): Sigma-Aldrich Sure/Seal 294829.

2.2 | *Ex vivo* incubations of human stool samples

Stool from four human donors (Table S1), previously frozen at −80°C upon collection, was aliquoted into a pre-equilibrated cryovial, weighed, diluted in reduced BHI^{CHV} at 10 mL per 1 gram of stool (0.1 g/mL), and vortexed to homogenize. Each sample was allowed to settle for 5 min and 100 μL of the sediment-free supernatant aliquoted into a new pre-equilibrated cryovial. Growth was evaluated by inoculating sterile BHI^{CHV} with 1:10 dilution of this fecal slurry, with OD_{600} readings performed every 15 min for 48 h with a 1-min shake prior to each absorbance reading at 37°C using an Eon Microplate Spectrophotometer (Biotek Instruments, Inc.). Simvastatin dilutions were made from a freshly prepared base stock of 2.5 mg/mL in DMSO. Samples were treated with either simvastatin (25 and 12 μg/mL) or an equal volume of 4% DMSO in a final volume of 100 μL prior to placing in the plate reader. Each donor's stool inoculation and treatment were evaluated

in triplicate (3 replicates per treatment group, Table S2). Samples were collected at the experimental endpoint to perform 16S rRNA gene sequencing (16S-seq) and analysis. All work described above were carried out in an anaerobic COY chamber. Growth curves were averaged by treatment and individual, and growth parameters (time to mid-exponential, carrying capacity, and growth rate) were estimated using the Growthcurver package (Sprouffske and Wagner, 2016). ANOVA was used to determine changes in growth parameters between groups. The maximal intestinal concentration of simvastatin was calculated as previously described (Zou et al., 2020): 40 mg recommended daily dose (source: simvastatin package insert) divided by 250 mL. Distal gut levels were estimated based on isotope labeling experiments indicating that 60% of the administered dose is excreted in stool (Wishart et al., 2018) (DrugBank accession: DB00641).

2.3 | 16S-seq and analysis of *ex vivo* incubations with simvastatin

Bacterial pellets from the *ex vivo* incubations above (100 µL) were collected by centrifugation at 3000 rpm for 5 min and then stored at −80°C. DNA was extracted using a ZymoBIOMICS 96 MagBead DNA Kit (Zymo D4308) as per the manufacturer's protocol, and 16S rRNA amplicon library was constructed following a dual-indexing approach (Gohl et al., 2016). Samples underwent 16S rRNA gene amplification using GoLay-barcoded V4 region V4-515F and V4-806R primers (Gohl et al., 2016) on a BioRad CFX 384 real-time PCR instrument with four serial 10 fold dilutions of extracted DNA template. Individual sample dilutions in the exponential phase were manually selected for subsequent indexing PCR using a dual GoLay index primers to add flow cell adaptors and indices as previously described (Gohl et al., 2016). DNA concentration was measured using a PicoGreen assay (P7589, Life Technologies) and samples were pooled at equimolar concentrations. Pooled libraries were purified and concentrated with MinElute PCR Purification kit (Qiagen #28004), run on 1% gel, size-selected (~427 bp), and purified using MinElute Gel Extraction kits (Qiagen, #28604). Libraries were quantified (NEBNext Library Quantification Kit; New England Biolabs) and sequenced with a 600 cycle MiSeq Reagent Kit v3 (paired-end reads set up for 250-bp in length; Illumina MiSeq) with 15% PhiX spiked in before sequencing at the UCSF Center for Advanced Technology.

QIIME2 (Bolyen et al., 2019) was used to trim primer reads, denoise the data, and create a feature table using the following: *qiime cutadapt trim-paired*, *qiime dada2 denoise-paired*, and *qiime feature-classifier classify-sklearn* as in our lab pipeline (https://github.com/jbisanz/16Spipelines/blob/master/QIIME2_pipeline.Rmd). Taxonomy was assigned using DADA2 (Callahan et al., 2016) with implementation of the RDP classifier (Wang et al., 2007) using the DADA2-formatted SILVA v128 training set. A phylogenetic tree was constructed using QIIME2 and the command *phylogeny align-to-tree-mafft-fasttree*. QIIME2 artifacts were imported into R using the qiime2R package (https://github.com/jbisanz/qiime2R). Low abundance taxa present in less than 3 samples and with less than 10 reads were filtered out. We assigned a unique ASV identifier that can be used to look up a full taxonomic assignment, from kingdom to species, associated with a sequence variant. Diversity metrics were generated using vegan (Dixon, 2003) and phyloseq (McMurdie & Holmes, 2013) packages in R. Principal coordinates analysis (PCoA) or Principal components analysis (PCA) were performed with ape (Paradis et al., 2004) or vegan packages, respectively. Analyses were carried out using the centered $\log_2$-ratio (CLR) normalized taxonomic abudances $A_{clr} = [\log_2(A_1/g_a), \log_2(A_2/g_a), \ldots \log_2(A_n/g_a)]$, where A is a vector of read counts with a prior of 0.5 added and g_a is the geometric mean of all values of A. Taxa were merged at different taxonomic levels using *tax_glom* from the phyloseq package before being CLR transformed where applicable. PERMANOVA was employed to detect changes in community composition from rarified counts or Bray-Curtis distances. Differential abundant ASVs were determined by employing ALDEx2 (Fernandes et al., 2013, 2014) using 150 simulations.

2.4 | *In vitro* bacterial growth studies

The isolates used in this study are found in Table S3. 37/39 of the tested isolates are commonly found in the human gut microbiota. Each of these strains was obtained from the Deutsche Sammlung von Mikroorganismen und Zellkulturen (DSMZ) culture collection. A single colony of each isolate was subcultured in 5 mL of BHI^{CHAV} for 48 h in an anaerobic chamber (Coy Laboratory Products) at 37°C with an atmosphere composed of 2%–3% H_2, 20% CO_2, and the balance N_2. This subculture was diluted down to an OD_{600} of 0.1, which was then further diluted 100-fold, and then used to inoculate a microtiter plate with 2-fold serial dilutions of simvastatin concentrations ranging from 1.5625 to 100 µg/mL or a 4% DMSO/MeOH vehicle control in a final volume of 100 µL. DMSO was used as a vehicle control for most of the isolates, except for the isolates from the Actinobacteria phylum, which we found did not tolerate DMSO well and MeOH was used instead. Higher concentrations of simvastatin were not tested due to solubility limits in BHI^{CHAV}. Plates were incubated at 37°C for 48 h in the anaerobic chamber and growth assessed by a final OD_{600} measurement. The minimal inhibitory concentration (MIC) was measured as the lowest concentration of simvastatin resulting in >90% growth inhibition after 48 h of incubation. Absorbance of cultures in 96-well plates were read using an Eon Microplate Spectrophotometer (BioTek Instruments, Inc).

2.5 | Tree construction

Full-length ribosomal sequences for each isolate were extracted from the database greengenes (DeSantis et al., 2006). Sequences were imported into Unipro UGENE (Okonechnikov et al., 2012) and aligned using MUSCLE (Edgar, 2004). Gaps occurring in >50% of sequences were removed and a maximum likelihood tree generated using PhyML (Guindon et al., 2010). For trees generated from

16S-seq from *ex vivo* samples, we used the ggtree R package (Yu et al., 2018).

2.6 | Bacterial incubations for transcriptional profiling

Bacterial isolates *E. lenta* DSM 2243 and *B. thetaiotaomicron* DSM 2079 were grown anaerobically in previously equilibrated BHI^{CHAV} at 37°C. Cultures for each isolate were grown to mid-exponential phase, split into triplicates, and incubated for 15 min at a range of simvastatin concentrations (1X, 0.5X, and 0.1X MIC; Table S3) or vehicle. Following incubations, cultures were removed from the anaerobic chamber in sealed Falcon tubes and placed immediately on ice. Cultures were centrifuged at 3000 rpm for 5 min at 4°C, the supernatant removed, and the bacterial pellets flash-frozen in liquid nitrogen for future RNA extraction.

2.7 | RNA extraction

Each bacterial pellet was incubated with 1 mL of Tri Reagent (Sigma Aldrich T9424) at room temperature for 10 min. The cell suspension was transferred into Lysing Matrix E tubes (MP Biomedicals, 116914050) and homogenized in a bead-beater (Mini-Beadbeater-24, BioSpec) for 5 min at room temperature. The sample was incubated with 200 μL of chloroform at room temperature for 10 min, followed by centrifugation at 16,000 *g* for 15 min at 4°C. Next, 500 μL of the upper aqueous phase was transferred into a new tube and 500 μL of 100% ethanol was added. To isolate RNA, we used the PureLink RNA Mini Kit (Life Technologies, catalog #: 12183025). This mixture was transferred onto a PureLink spin column and spun at ≥12,000×*g* for 30 s. The column was washed with 350 μL of wash buffer I as described in the PureLink manual. The column was incubated with 80 μL of PureLink DNase (Life Technologies, catalog #: 12185010) at room temperature for 15 min, and washed with 350 μL of wash buffer I. The column was washed with wash buffer II twice as described in the PureLink manual. Total RNA was recovered in 50 μL of RNase-free water. A second round of DNAse treatment was undertaken. The RNA was incubated with 6 μL of TURBO DNAse (Ambion, ThermoFisher, catalog #: AM2238) at 37°C for 30 min. To stop the reaction, 56 μL of lysis buffer from the PureLink kit and 56 μL of 100% ethanol was added to the sample and vortexed. This suspension was transferred onto a PureLink column and washed once with 350 μL of wash buffer I and twice with 500 μL of wash buffer II. The RNA was recovered in 30 μL of RNAse-free water.

2.8 | rRNA depletion, library generation, and RNA sequencing

Total RNA was subjected to rRNA depletion using the RiboMinus Bacteria Transcription Isolation kit (ThermoFisher, catalog # A47335), following the manufacturer's protocol. RNA fragmentation, cDNA synthesis, and library preparation proceeded using NEBNext Ultra RNA Library Prep Kit for Illumina (New England BioLabs, catalog # E7530) and NEBNext Multiplex Oligos for Illumina, Dual Index Primers (New England BioLabs, catalog # E7600), following the manufacturer's protocol. All samples were paired end sequenced (2 ×150 bp) using an Illumina NovaSeq platform (NovaSeq 6000 v1.5) at the UCSF Institute for Human Genetics.

2.9 | RNA sequencing analysis

Reads were trimmed using fastp (Chen et al., 2018). Reference genomes were obtained from NCBI's genome assembly database under the following accession numbers: ASM2426v1 for *E. lenta* and ASM1106v1 for *B. thetaiotaomicron*. Reads were mapped to reference genomes using Bowtie2 (Langmead & Salzberg, 2012) using the following options: *q*, *--met-file*, *--end-to-end*, *--sensitive*. HTSeq (Anders et al., 2014) was used to count the number of transcripts mapping to genes using the following options: *--type*=CDS, *--idattr*:ID, *--stranded*=no, *--minaqual*=10. Differential abundance of gene transcripts in the simvastatin treated (low, med, high) and untreated samples was assessed using DESeq2 (Love et al., 2014) (v1.26.0) with the *DeSeqDataSetFromHTSeqCount* and *ddsHTSeq* functions and their default options. Different FDR thresholds ranging from 0.01 to 0.1 were used to determine the number of differentially expressed genes, and irrespective of the threshold used, consistent percentages of each bacterial genome were affected by simvastatin. Ultimately, a threshold of FDR < 0.1 and $|\log_2$ fold-change$| > 1$ was chosen to determine significance. BlastKOALA (Kanehisa et al., 2016) was used to map protein sequences from each organism to KO terms using the "species_prokaryote" database. KEGG pathway enrichment was carried out using clusterProfiler (Yu et al., 2012) (v3.14.3) and the enrichKEGG function. KO terms for all differentially abundant barcodes (both up- and down-regulated with a $p_{adj} < 0.1$, DESeq2 and $|\log_2$ fold-change$| > 1$) were provided and the organism parameter was set to "ko". Heatmaps and volcano plots were generated using the ggplot2 R package (Wickham, 2016) (v3.3.5).

2.10 | *In vitro* transposon mutant fitness assays and barcode sequencing

We performed *B. thetaiotaomicron* transposon mutant fitness assays as described previously (Liu et al., 2021). For *B. thetaiotaomicron*, we thawed an aliquot of the full transposon mutant library, inoculated the entire aliquot into 50 mL of BHI^{CHV} supplemented with 10 μg/mL erythromycin, and grew the library to mid-log phase. We then collected 6 cell pellets of ~1.0 OD_{600} unit each (the "Time0" sample). We used the remaining cells to inoculate competitive growth assays in the presence of simvastatin or a vehicle control. All fitness assays were performed in 1.2 mL of growth medium in a 24-well transparent microplate (Greiner) at a starting OD_{600} of 0.02. We

grew cultures until the vehicle group reached stationary phase and then collected cell pellets (the "Condition" sample). We extracted genomic DNA from the Time0 and Condition samples in a 96-well microplate format with a ZymoBIOMICS 96 MagBead DNA kit (ZymoResearch, catalog # D4302). We performed barcode sequencing (BarSeq) as previously described (Liu et al., 2021; Price et al., 2018). We used BarSeq oligos with both P1 and P2 indexed to minimize the impact of incorrectly assigned indexes in Illumina HiSeq4000 runs (Sinha et al., 2017). Strain and gene fitness scores were calculated as previously described and can be found within the Fitness Browser (https://fit.genomics.lbl.gov) (Wetmore et al., 2015). Fitness values are $\log_2$ ratios that describe the change in abundance of mutants in that gene during the experiment. For most of the fitness experiments, which are growth experiments, the change reflects how well the mutants grow relative to the "Time0" samples. The "Time0" samples also serve as a control to ensure the number of mutants across an experiment are consistent with previous fitness assays.

2.11 | Transposon sequencing analysis

Barcoded transposon insertions were summed for each gene. Differential abundance of the individual genes in the treated and untreated mutant populations was assessed using DESeq2 (Love et al., 2014) (v1.26.0) with the *DeSeqDataSetFromMatrix* and *dds* functions and their default options on the gene count matrix. A threshold of FDR < 0.1 and $|\log_2$ fold-change$| > 1$ was used to determine significance. BlastKOALA (Kanehisa et al., 2016) was used to map protein sequences from each organism to KO terms using the "species_prokaryote" database. KEGG pathway enrichment was carried out using clusterProfiler (Yu et al., 2012) (v3.14.3) using the enrichKEGG function. KO terms for all differentially abundant barcodes (both up- and down-regulated with a FDR < 0.1, DESeq2 and $|\log_2$ fold-change$| > 1$) were provided and the organism parameter was set to "ko". Heatmaps and volcano plots were generated using the ggplot2 R package (Wickham, 2016) (v3.3.5).

2.12 | Comparative genomics

A previous pan-genome analysis (Bisanz et al., 2020) was used to assess conservation of marR genes across gut Coriobacteriia isolate genomes defined using ProteinOrtho v6.0.6 (Lechner et al., 2011), with gene family cutoffs of 60% identity and 80% coverage. marR gene families were defined based on annotation of the *E. lenta* DSM 2243 genome using InterProScan (Zdobnov & Apweiler, 2001). Our results were largely unchanged when using a looser sequence identity cutoff (40%). The United Human Gastrointestinal Genome collection (v2.0.1) was used to assess conservation of tolC-like systems across human gut microbes. The 4,744 species representative genomes and corresponding eggNOG-db annotations (Huerta-Cepas et al., 2019) were downloaded from the MGnify database (https://www.ebi.ac.uk/metagenomics/browse/genomes), including 619 assigned to the Bacteroidota phylum (91 isolates and 528 metagenome-assembled genomes) (Gurbich et al., 2023). The following phylum-level eggNOG gene families were used to define the *B. thetaiotaomicron*-like tolC gene cluster: 4NEXN (BT_3339), 4NDZG (BT_3338) and 4NDZK (BT_3337). All 3 gene families were required to be adjacent to each other to be counted as a complete system, as in the *B. thetaiotaomicron* genome. The following phylum-level eggNOG gene families were used to define the *Escherichia coli*-like tolC genes in Proteobacteria: 1MU78 (b0463), 1MU48 (b0462), and 1MWCJ (b3035). These were not required to be adjacent.

3 | RESULTS

3.1 | Simvastatin directly inhibits gut bacterial growth in mixed and pure cultures

We used our established methods for the *ex vivo* incubation of the human gut microbiota (Maurice et al., 2013; Nayak et al., 2021) to test the impact of simvastatin on gut microbial community structure in the absence of a host. Stool samples were selected from ImmunoMicrobiome cohort, an ongoing study of the microbiome and immune system of healthy participants (Table S1). Growth was tracked longitudinally for 48 h by optical density and 16S rRNA gene sequencing (16S-seq) was performed at the experimental endpoint (Table S2). The simvastatin concentrations tested (≤25 μg/mL) were below the estimated maximum intestinal concentration (160 μg/mL) even after accounting for absorption in the proximal gut (96 μg/mL in stool).

Simvastatin had a significant impact on the gut microbiota across multiple metrics. Analysis of our growth curves revealed a dose-dependent delay in the overall growth of the human gut microbiota, resulting in a significant increase in the time it took to reach mid-exponential phase (Figure 1a). Community-wide carrying capacity and growth rate trended lower in response to simvastatin, but did not reach statistical significance potentially due to insufficient power (Figure S1a,b). We also observed a significant and dose-dependent decrease in microbial diversity, as assessed by the Shannon diversity index (Figure 1b) and the number of amplicon sequence variants (ASVs; Figure S1c). Consistent with prior studies (Maurice et al., 2013), analysis of the full 16S-seq dataset revealed marked inter-individual variations in the gut microbiota with a slight convergence based on simvastatin concentration (Figures 1c and S1d). After stratifying the data by subject, we observed clear and statistically significant effects of simvastatin on gut microbial community structure (Figure 1d). At the phylum level, simvastatin significantly decreased Bacteroidota and increased Verrucomicrobiota (Figure 1e). Significant differences were also apparent at the ASV level, including 7 depleted ASVs and 3 enriched ASVs (Figure 1f). With the exception of an ASV identified as *Eggerthella lenta*, the remaining 6 depleted ASVs were significantly affected at both doses of simvastatin. An ASV identified as *Bacteroides thetaiotaomicron* was the most dramatically depleted ASV, with a 9-fold reduction in

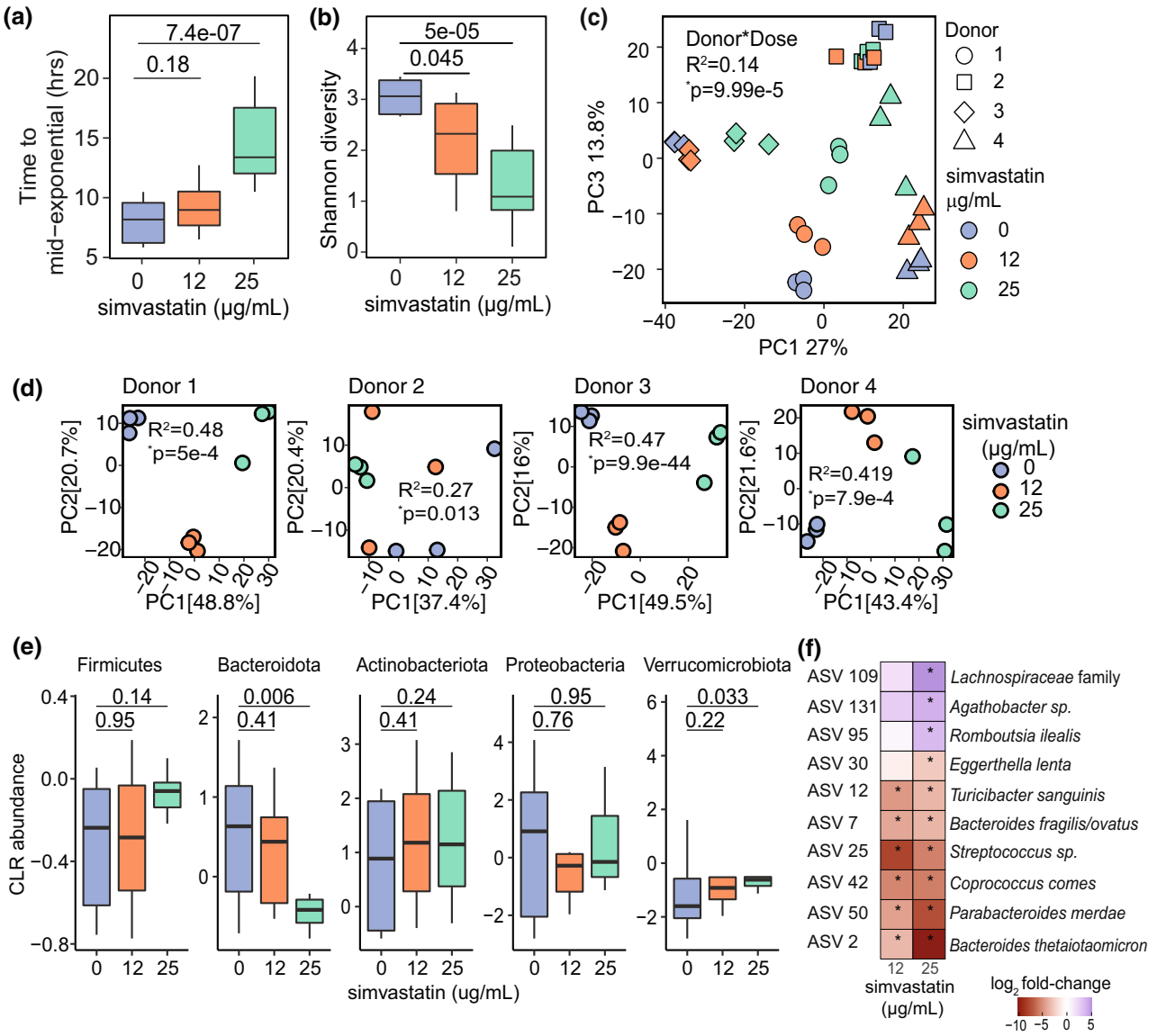

FIGURE 1 Simvastatin directly alters the growth and community structure of the human gut microbiota. Human *ex vivo* stool cultures ($n=4$ donors, $n=3$ biological replicates/concentration; Table S1) were grown with simvastatin or a vehicle control for 48 h and analyzed by 16S rRNA gene sequencing (Table S2). (a) Time to mid-exponential growth in hours from the growth data. (b) Bacterial diversity decreases as the concentration of simvastatin increases based on the Shannon diversity index. (c) Principal components 1 and 3 of Euclidean distances using center $\log_2$-ratio (CLR)-transformed values from 16S-seq data colored by simvastatin concentration and shaped by donor sample to facilitate the visualization of their effects. (d) Principal components 1 and 2 of Euclidean distances using CLR-transformed values from 16S-seq data calculated for each donor. (e) Taxonomic data from all samples aggregated at the phylum-level, CLR-transformed, and compared across simvastatin concentrations. (f) ASVs differentially abundant across all samples in response to simvastatin at 25 µg/mL that also show consistent directionality in response to simvastatin at 12 µg/mL (ALDEx2 comparing samples treated with each simvastatin concentration relative to the vehicle). Colors indicate the difference in CLR-transformed values between simvastatin and vehicle groups. Boxplots in panels a, b, e: top and bottom hinges are the first and third quartiles, horizontal lines denote the median, and whiskers extend to the maximum and minimum values. *p*-values represent Wilcoxon rank-sum tests (panels a,b,e; *p-value <0.05, panel f) or PERMANOVA tests (panels c and d) between treatment groups.

abundance. Taken together, these results show that simvastatin has a dramatic effect on the human gut microbiota in the absence of a host.

Next, we sought to gain a more precise understanding of the growth inhibitory properties of simvastatin on human gut bacteria grown in isolation. We leveraged a previously generated collection of 39 human gut bacterial strains spanning 5 phyla (Table S3) (Nayak et al., 2021; Spanogiannopoulos et al., 2022). Each strain was grown in rich media (brain heart infusion with supplements; BHI^{CHAV}), which we previously showed supports the robust growth of this entire collection (Spanogiannopoulos et al., 2022). Simvastatin was included at a range of concentrations (1.56–100 µg/mL) at or below the estimated distal gut concentration (96 µg/mL). Most of the tested strains (30/39) had a measurable MIC (defined by a 90%

decrease in carrying capacity), which ranged from 25 to 100 μg/mL (Figure 2 and Table S3). Of the strains with a measurable MIC, members of the Firmicutes and Actinobacteriota phyla had a significantly higher MIC relative to members of the Bacteroidota phylum (Figure S2). Within the tested Actinobacteriota, simvastatin sensitivity varied >3-fold, with *Collinsella aerofaciens* and *Bifidobacterium longum* tolerating higher levels than *E. lenta* and the other *Coriobacteriaceae*. Of note, both *B. thetaiotaomicron* and *E. lenta* were consistently affected by simvastatin in the context of a complex community and pure cultures. This fact, together with our extensive tools for *B. thetaiotaomicron* genetics (Liu et al., 2021) and *E. lenta* functional genomics (Bisanz et al., 2020) led us to focus on these two bacteria for more in-depth analysis.

3.2 | *E. lenta* upregulates genes for membrane biogenesis in response to simvastatin

Given the lack of variation in simvastatin sensitivity within the *Eggerthellaceae* (Table S3), we turned to transcriptional profiling (RNA-seq) to gain insights into the genes and metabolic pathways altered in response to simvastatin. We grew *E. lenta* in rich media and added 3 concentrations of simvastatin [low, med, high; 0.1–1X MIC] or vehicle controls at mid-exponential growth. Samples were collected 15 min later and used for RNA-seq and analysis (Table S4).

Simvastatin induced a substantial change in *E. lenta* gene expression. Principal components analysis revealed clear grouping of the overall transcriptomes of the two higher doses relative

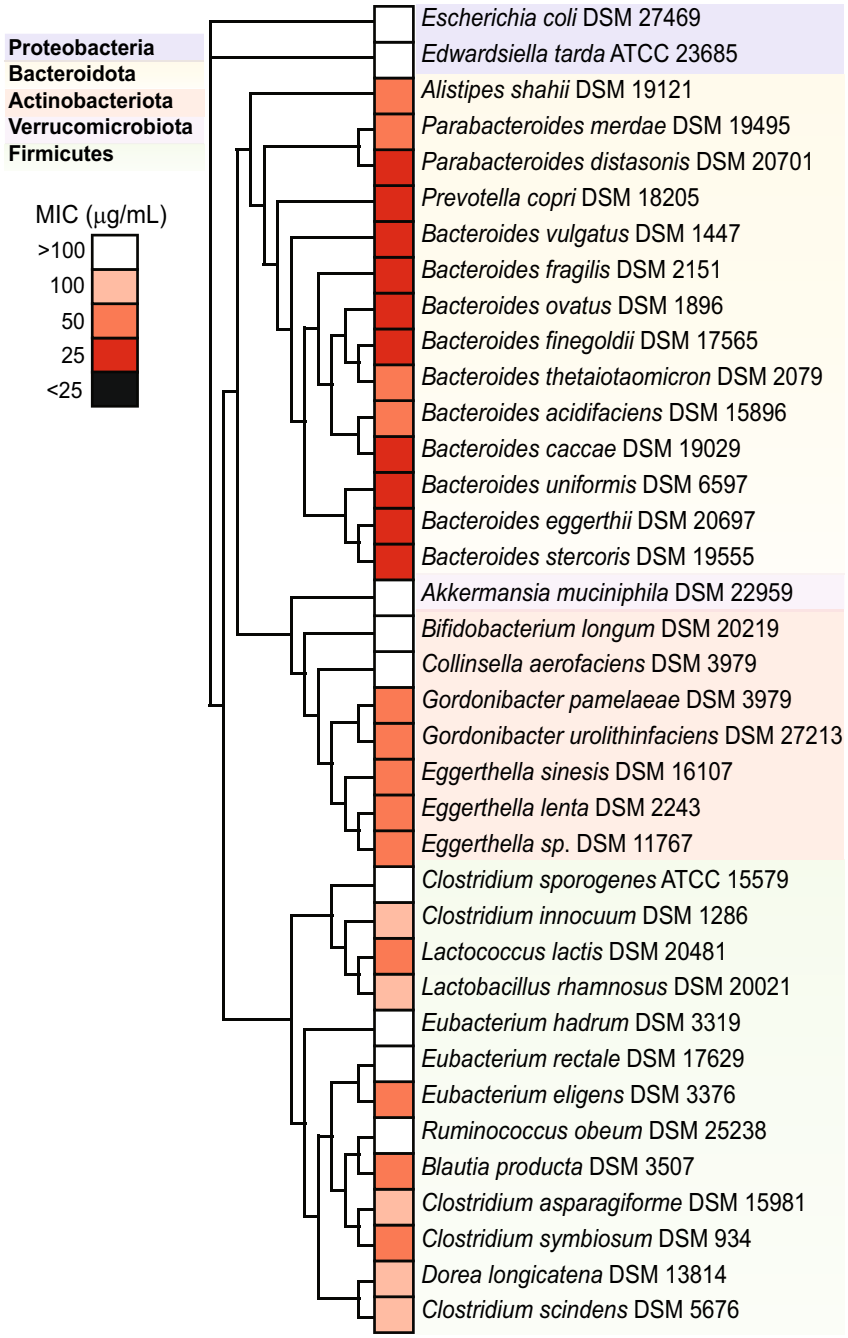

FIGURE 2 Simvastatin directly inhibits the growth of human gut bacterial isolates. A diverse panel of 39 representative gut bacterial strains (Table S3) were incubated with varying concentrations of simvastatin (1.56–100 μg/mL in 2-fold increments, $n = 3$ biological replicates/concentration tested) and the MIC determined. A phylogenetic tree using full-length 16S rRNA gene sequences for each organism was constructed. MIC, minimum inhibitory concentration. The tree shows 37 of the isolates (2 additional *Eggerthella* strains were tested but only one of each species was included in the tree).

to the lowest dose and vehicle controls (Figure 3a). These differences were statistically significant ($R^2 = 0.393$ and $p = 0.046$, PERMANOVA; comparing simvastatin doses to vehicle controls). The number of differentially expressed genes (FDR < 0.1 and |$\log_2$ fold-change| > 1, DESeq2) was dose-dependent (Figure 3b and Table S5), ranging from 2 to 250 upregulated and 0 to 240 downregulated genes relative to vehicle controls. At the highest dose, 16% (490/3,086) of *E. lenta* protein-coding genes were differentially expressed. The set of differentially expressed genes was dose-dependent, with 294 genes unique to the highest dose (Figure 3c). Pathway enrichment analysis demonstrated that the two higher doses of simvastatin consistently impacted 7 genes involved in fatty acid biosynthesis important for building lipids used in the cell membrane (Figure 3d).

Interestingly, we observed 4 simvastatin-dependent genes annotated in NCBI as multiple antibiotic resistance transcriptional regulators (MarRs) (Sulavik et al., 1995). MarRs typically repress their own promoter (Grove, 2013; Perera and Grove, 2010). Ligand binding releases MarR from the promoter, inducing expression of MarR and neighboring genes (Figure 4a). MarR has been implicated in stress responses as well as the degradation/export of phenolic compounds and antibiotics (Grove, 2013). MarRs can bind to diverse ligands, including the antibiotics kanamycin, salicylate, and 2,4-dinitrophenol (Grove, 2013; Lomovskaya et al., 1995; Perera & Grove, 2010; Xiong et al., 2000), but direct binding to statins has not been reported.

In total, the *E. lenta* genome contains 9 MarR homologs, of which 4 are upregulated with a high dose of simvastatin. These 4 gene clusters have diverse functions including ATP-binding cassette (ABC) drug transport, heat shock response, fatty acid biosynthesis, and multidrug and toxic compound extrusion (Figure 4b). Of note, one of these putative MarR-regulated clusters encodes 6 genes involved in fatty acid biosynthesis (Figure 4b), all of which are induced at the two higher doses of simvastatin, consistent with our pathway

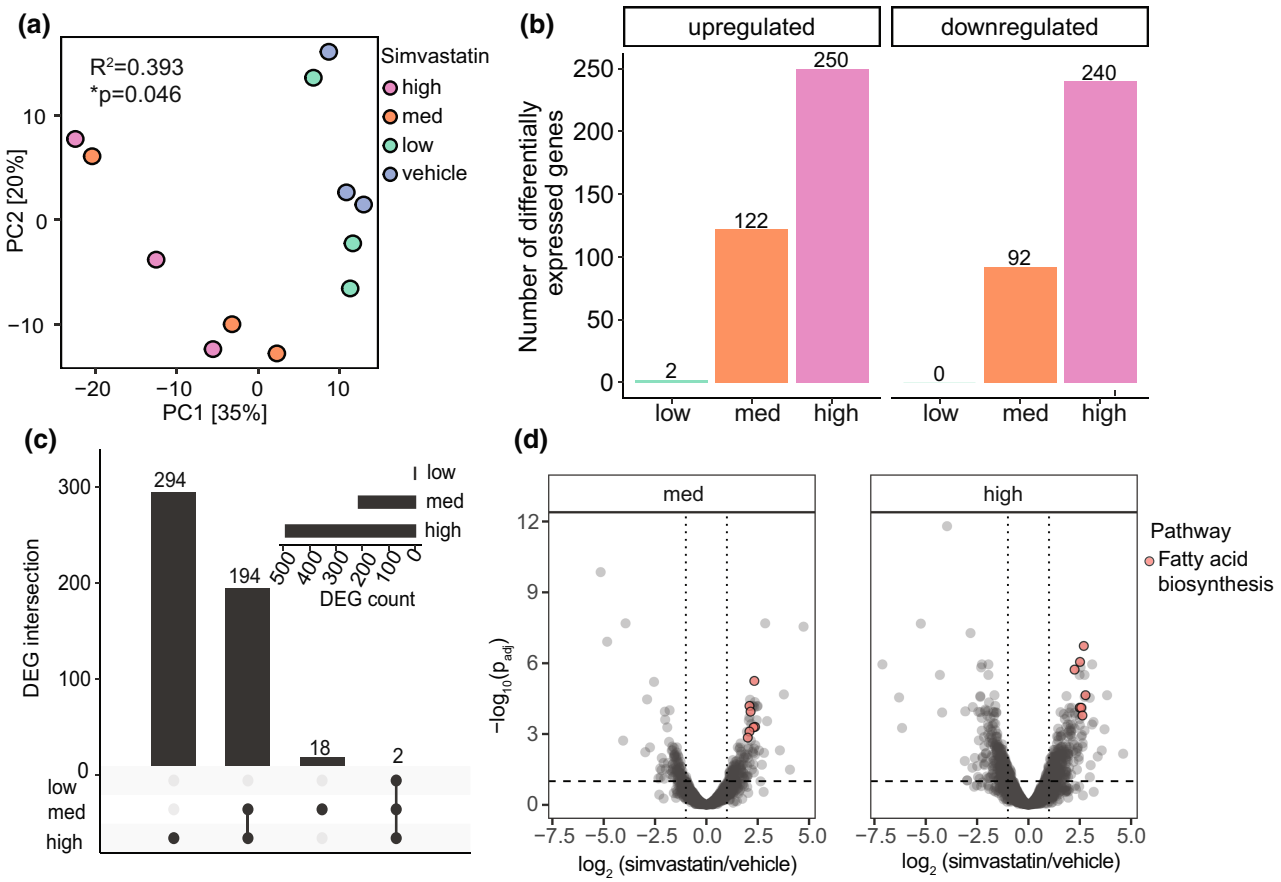

FIGURE 3 Simvastatin has a dose-dependent effect on the *E. lenta* transcriptome and induces genes for cell membrane integrity. (a) PCA of *E. lenta* DSM 2243 RNA-seq data comparing three doses of simvastatin to vehicle controls: low, low-dose (6 μg/mL); med, medium-dose (30 μg/mL); high, high-dose (60 μg/mL). Statistical results of PERMANOVA are reported ($n = 3$ biological replicates/group, Tables S4 and S5). (b) Number of differentially expressed genes (DEGs; FDR < 0.1 and |$\log_2$ fold-change| > 1, DESeq2) comparing each simvastatin dose relative to vehicle controls. (c) Overlap between DEGs across simvastatin doses. (d) Volcano plot of the medium and high simvastatin doses relative to vehicle controls: horizontal line, |$\log_2$ fold-change| > 1; vertical line, FDR < 0.1. Colored points represent fatty acid biosynthesis pathway genes found to be significantly enriched by a KEGG pathway enrichment using clusterProfiler ($p_{adj} < 0.2$, Benjamini–Hochberg correction). The KEGG overview map for fatty acid metabolism (KEGG map01212), which the fatty acid biosynthesis pathway falls under, was also significantly enriched due to an overlapping set of genes between them.

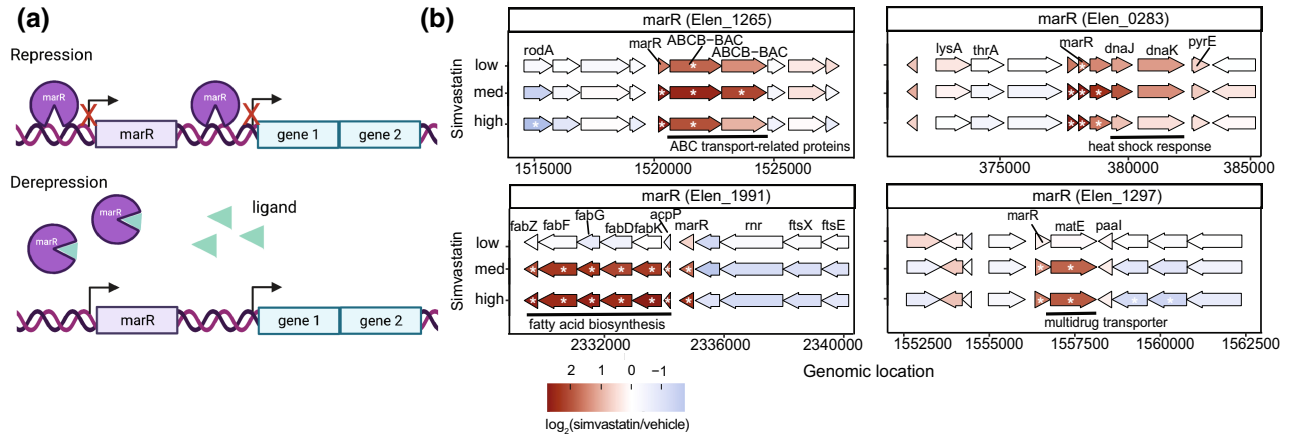

FIGURE 4 Simvastatin induces multiple MarR-dependent gene clusters in *E. lenta*. (a) Diagram of a marR and its mode of gene regulation (created with BioRender.com). MarR acts as a transcriptional repressor of itself and neighboring gene clusters by binding to site-specific DNA regions upstream. When MarR is bound to a ligand, repression is released and allows for the transcription of previously repressed genes (Grove, 2013). (b) Locus diagram showing the 4 differentially expressed *marR* genes (FDR < 0.1 and $|\log_2$ fold-change$| > 1$, DESeq2) and their adjacent gene clusters across different doses of simvastatin. Colors are $\log_2$ fold-changes relative to vehicle controls. Significance is represented with an asterisk. Gene and gene cluster annotations shown where available.

enrichment analysis (Figure 3d). Taken together, these results support a working model in which simvastatin either directly or indirectly affects *E. lenta* MarR, lifting its repression of multiple gene clusters, including a suite of genes that are predicted to alter cell membrane lipid composition. Notably, all 9 MarR genes are also conserved across the *E. lenta* species, supporting their core importance for stress response (Figure S3).

3.3 | *B. thetaiotaomicron* upregulates efflux systems that protect against simvastatin

Next, we sought to assess the similarities and differences in simvastatin response in another drug sensitive bacterium. We selected *B. thetaiotaomicron* due to its robust genetic tools (Liu et al., 2021) and to compare a Gram-negative bacterium to the Gram-positive *E. lenta*. As done previously for *E. lenta*, we grew *B. thetaiotaomicron* to mid-exponential phase then added 3 concentrations of simvastatin [low, med, high; 0.1–1X MIC] or vehicle controls at mid-exponential growth. Samples were collected 15 min later and used for RNA-seq and analysis (Table S4).

Remarkably, *B. thetaiotaomicron* exhibited an even more dramatic transcriptional response to simvastatin than *E. lenta*. Principal components analysis revealed clear grouping of the overall transcriptomes of all three doses relative to vehicle controls (Figure 5a); all three doses were statistically significant relative to vehicle controls ($R^2 = 0.47$ and $p = 0.003$, PERMANOVA; comparing simvastatin doses to vehicle controls). The number of differentially expressed genes (FDR < 0.1 and $|\log_2$ fold-change$| > 1$, DESeq2) was higher than *E. lenta* overall but still dose-dependent (Figure 5b and Table S6), ranging from 115 to 473 upregulated and 8 to 468 downregulated genes relative to vehicle controls. At the highest dose, 19% of *B. thetaiotaomicron* genes (879/4,650) were differentially expressed. Thirty-one differentially expressed genes were independent of dose, whereas 619 were consistently altered at the two higher doses (Figure 5c). Pathway enrichment analysis demonstrated a dose-independent enrichment for differentially expressed genes involved in oxidative phosphorylation (Figure 5d). The highest dose also affected genes involved in histidine, glyoxylate/dicarboxylate, and galactose metabolism pathways, whereas the lowest dose affected genes involved drug (beta-lactam) resistance and the TCA cycle (Figure 5d).

Interestingly, many of the top differentially expressed genes encoded the subunits of 3 distinct multidrug efflux systems (Figures 6a,b). All of these systems are homologous to the AcrAB-TolC system in *Escherichia coli* (Table S7), which enables the efflux of a wide variety of compounds, including antibiotics (Li and Nikaido, 2009). Similar to *E. coli*, each efflux system in *B. thetaiotaomicron* includes three major subunits, all of which are differentially expressed in response to simvastatin: (i) the hydrogen-dependent inner membrane transporter AcrB; (ii) the periplasmic membrane fusion protein AcrA; and (iii) the outer membrane channel protein TolC (Li & Nikaido, 2009). Gene order is conserved in the 3 putative *B. thetaiotaomicron* AcrAB-TolC efflux systems (Figure 6d). Although the *B. thetaiotaomicron* systems remain uncharacterized at the biochemical level, we recently used transposon mutagenesis to implicate one of the 3 systems (encoded by the genes BT3337-9; referred to herein as AcrAB-TolC1) in resistance to the antibiotics fusidic acid and cefoxitin, and the antipsychotic chlorpromazine (Liu et al., 2021).

To test the impact of all three efflux systems on growth in the presence of simvastatin, we turned to our previously published barcoded transposon sequencing library (Liu et al., 2021). This barcoded transposon mutant library carries transposon insertions in 4,055 non-essential genes whose change in abundance can be measured in the presence of a stressor, previously described as a genome-wide

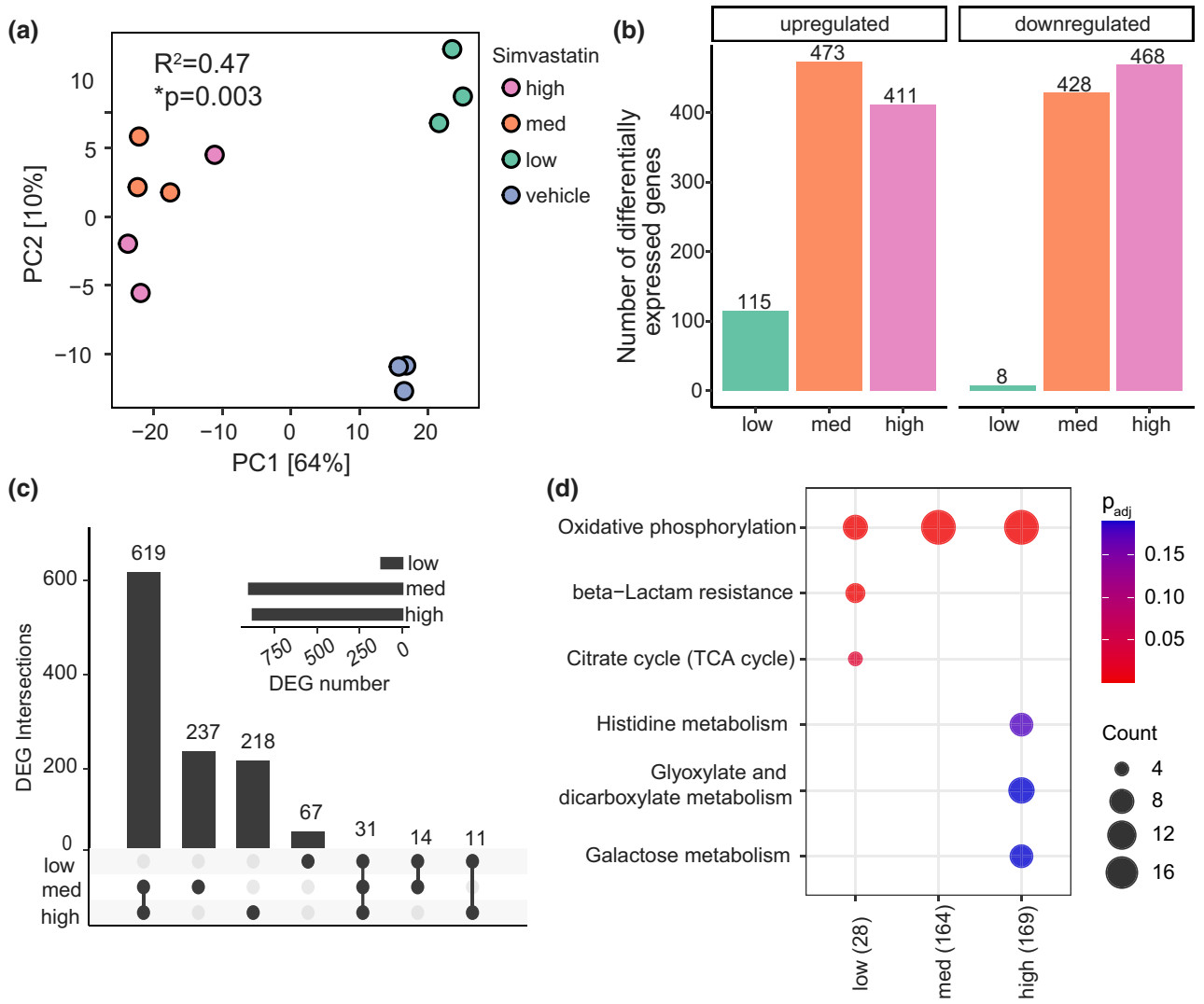

FIGURE 5 Simvastatin has a dose-dependent effect on the *B. thetaiotaomicron* transcriptome. (a) PCA of *B. thetaiotaomicron* DSM2079 RNA-seq data comparing three doses of simvastatin to vehicle controls: low, low-dose (5 μg/mL); med, medium-dose (25 μg/mL); high, high dose (50 μg/mL). Statistical results of PERMANOVA are reported ($n = 3$ biological replicates/group, Tables S4 and S6). (b) Number of differentially expressed genes (DEGs; FDR < 0.1 and $|\log_2$ fold-change$| > 1$ DESeq2) comparing each simvastatin dose relative to vehicle controls. (c) Overlap between DEGs across simvastatin doses. (d) KEGG pathway enrichments for DEGs ($p_{adj} < 0.2$, Benjamini–Hochberg correction): colors, $\log_{10} p_{adj}$; count, number of DEGs. (b–d) $n = 2$–3 biological replicates/group; one sample from the high dose simvastatin group was excluded due to low sequencing depth (Table S4).

fitness assay (Liu et al., 2021). We performed a fitness assay in which we grew up the transposon mutant library in the presence of low [0.1X MIC] levels of simvastatin or vehicle and then looked at the differential abundance of the gene insertions relative to the vehicle (Table S8). In total, we identified 102 genes that have significantly improved growth in simvastatin when disrupted and 117 genes whose insertions had significantly impaired growth (FDR < 0.1, $|\log_2$ fold-change$| > 1$, DESeq2; Table S9). The genes that exhibited increased growth upon transposon insertion included cardiolipin synthetase (BT3978, Table S9), potentially suggesting that cardiolipin incorporation into the inner membrane increases simvastatin sensitivity (Davlieva et al., 2013). On the other hand, we noted multiple genes important for simvastatin tolerance, including the transporter system encoded by BT3337-BT3339 (referred to herein as AcrAB-TolC1), important for fusidic acid tolerance (Liu et al., 2021) (Figure 6c).

We performed a more in-depth analysis of the three *B. thetaiotaomicron* AcrAB-TolC systems that we had previously identified by RNA-seq. The greatest fitness defect was observed when AcrAB-TolC1 was disrupted (Figures 6c,e and Table S9), consistent with its high level of baseline gene expression (Figure S4a). All three systems were significantly induced by low levels of simvastatin, with AcrAB-TolC2 and AcrAB-TolC3 showing the most dramatic upregulation (Figures 6b,d and S4a–c).

Follow-up experiments confirmed that the sensitivity of *B. thetaiotaomicron* to simvastatin was increased in response to chemical and genetic disruption of drug efflux. We used phenylalanine-arginine β-napthylamide (PAβN), which inhibits RND family drug

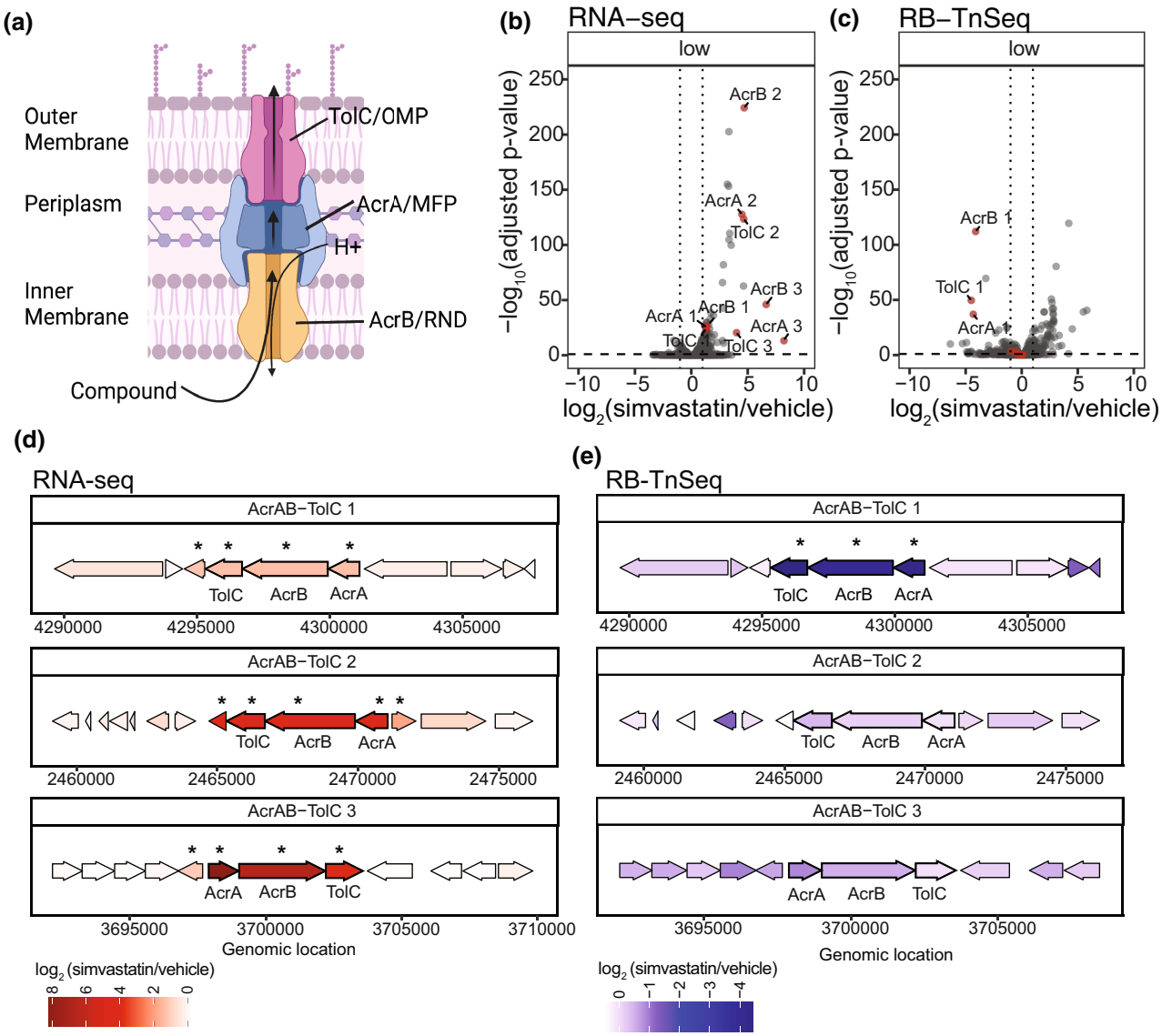

FIGURE 6 Simvastatin induces drug efflux systems in *B. thetaiotaomicron* that enable growth. (a) Schematic of a characterized Resistance-Nodulation-Division (RND) family efflux system (adapted from Anes et al., 2015). (b, c) Volcano plots of RNA-seq (b, Table S6) and RB-TnSeq (c, Table S9) following exposure of *B. thetaiotaomicron* to a low dose of simvastatin relative to vehicle controls (5 μg/mL, 0.1X MIC, $n = 3$ biological replicates/group). Genes homologous to the RND family efflux system BT3337-BT3339/AcrAB-TolC1 (Liu et al., 2021) are labeled red (Table S7). Points above the horizontal dotted line and to the right and left of the vertical dotted lines have an FDR < 0.1 and $|\log_2$ fold-change$| > 1$ (DESeq2). (d,e) Genomic loci in *B. thetaiotaomicron* containing RND efflux genes and neighboring genes. Asterisks indicate genes differentially abundant in the presence of simvastatin relative to vehicle controls. (b–e) AcrAB-TolC1 refers to BT3337-BT3339; AcrAB-TolC2 refers to BT1965-1967; AcrAB-TolC3 refers to BT2940-BT2942 (Tables S7 and S9).

efflux systems, including AcrAB-TolC (Lamers et al., 2013). The *B. thetaiotaomicron* MIC for simvastatin significantly decreased in response to PAβN (Figure 7a). We obtained stocks with transposon insertions in each of the three *B. thetaiotaomicron tolC* genes (Arjes et al., 2022). Transposon insertions in two of the loci (*tolC1::Tn* and *tolC3::Tn*) resulted in a lower MIC for simvastatin relative to *wt* (Figure 7b). These results are generalizable to other species; disruption of the single *tolC* encoded by *E. coli* (*ΔtolC::KanR*) led to a significant increase in simvastatin sensitivity (Figure 7c). Interestingly, while AcrAB-TolC systems are prevalent in members of the Bacteroidota and Proteobacteria, they vary in copy number; Bacteroidota strains can have a maximum of up to 7 systems (Figure S5a), while Proteobacteria have a maximum of 2 (Figure S5b). These results, together with another recent report (Maier et al., 2018), highlight the key role of multi-drug efflux systems in bacterial resistance to both antibiotics and host-targeted drugs.

4 | DISCUSSION

Our results demonstrate that simvastatin elicits a direct antibacterial effect on a broader range of human gut bacteria than previously

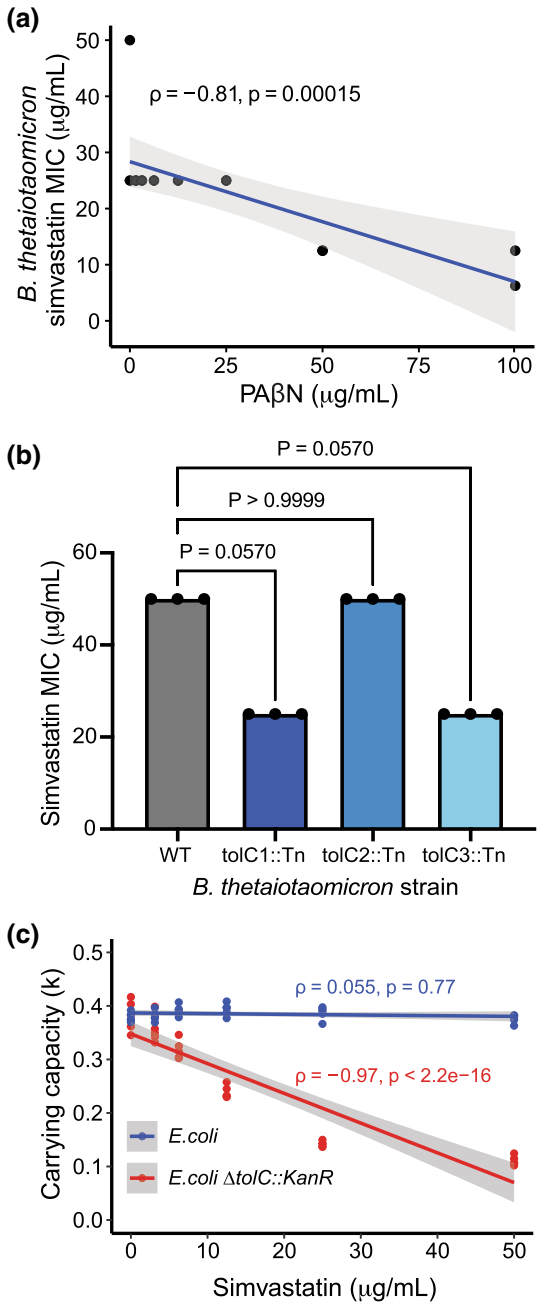

FIGURE 7 RND family drug efflux systems decrease simvastatin sensitivity in *B. thetaiotaomicron* and *E. coli*. (a) *B. thetaiotaomicron* simvastatin MIC is decreased in response to the efflux inhibitor PAβN (Spearman $\rho = -0.81$, $p = 0.00015$; $n = 2$ biological replicates/concentration). Regression line and 95% confidence interval are shown. (b) Transposon insertions in individual tolC genes decreases the MIC of simvastatin for *B. thetaiotaomicron*. (Kruskal–Wallis multiple comparison test; n = 3 biological replicates/concentration). (c) TolC protects *E. coli* from simvastatin. The *ΔtolC::KanR* strain exhibits significantly lower carrying capacity in response to increasing concentrations of simvastatin (Spearman $\rho = -0.97$, $p < 2.2e{-}16$; $n = 3$ biological replicates/concentration). Regression lines and 95% confidence intervals are shown.

appreciated (Ko et al., 2017; Maier et al., 2018). A prior *in vitro* screen identified a single dose of simvastatin (8.37 μg/mL, 20 μM) that affected the growth of 3 gut bacterial isolates (*P. distasonis*, *R. torques*, and *R. intestinalis*) in mono-culture (Maier et al., 2018). In this study, we expanded the list of simvastatin-sensitive strains by testing a range of physiologically relevant drug concentrations on human gut bacterial communities and a panel of gut bacterial isolates. Drug sensitivity varied in the context of a community versus pure culture. However, common trends in susceptibility to simvastatin were observed from the phylum- to strain-level. Members of the phylum Bacteroidota were on average more susceptible to simvastatin. A subset of strains from multiple phyla had consistent susceptibility to simvastatin when present in either a community or in isolation, including *B. thetaiotaomicron* and *E. lenta*, which we chose for more in-depth follow-up experiments.

It remains perplexing that simvastatin has direct antimicrobial effects given that HMG-CoA reductase, the canonical target of simvastatin, is rare in human gut bacterial genomes (Gill et al., 2006; Heuston et al., 2012). More work is needed to elucidate the mechanism(s) of action that leads to the observed inhibition of diverse gut bacterial species.

Our results indicate that simvastatin has a broad impact on gut bacterial gene expression. These results mirror our prior work on the antimetabolite drugs methotrexate and 5-fluorouracil, which demonstrate the marked effect drug exposure can have on gut bacterial transcriptional activity (Nayak et al., 2021; Spanogiannopoulos et al., 2022). This suggests that simvastatin either directly or indirectly alters the core metabolic pathways of gut bacteria which are often essential and not reflected in loss-of-function screens. A gain-of-function screen using a barcoded overexpression bacterial shotgun expression library sequencing (Boba-seq), might help complement some of our findings and has the advantage of capturing essential genes (Huang et al., 2022). Future studies utilizing affinity probes (Brandvold et al., 2021) or other chemical biology tools could help to identify proteins that directly interact with simvastatin within bacterial cells, complementing the bacterial genetic and transcriptomic tools used in this study.

The bacterial cell membrane and its changes in permeability from the incorporation of fatty acids play a key role in antibiotic resistance (Royce et al., 2013; Su et al., 2021). This has been established for antibiotics like ciprofloxacin (Su et al., 2021), but not for antibacterial statins. Here, we found that *E. lenta* responds to simvastatin via the upregulation of genes for fatty acid biosynthesis. More work is needed to explore exactly how the enhanced biosynthesis of fatty acids might contribute to simvastatin resistance. This can be studied by employing fatty acid biosynthesis inhibitors (Su et al., 2021) like triclosan and 2-aminooxazole in synergy with simvastatin to test how their combination affects simvastatin susceptibility and cell morphology.

We also found that a subset of transcriptional regulators from the MarR family are upregulated by *E. lenta* in response to simvastatin. MarR-type regulators generally respond to environmental stress responses, including stress triggered by antibiotics, by controlling a small set of genes often located in the same gene cluster (Lomovskaya et al., 1995; Poole et al., 1996; Srikumar et al., 2000; Xiong et al., 2000). In *E. lenta*, these MarR homologs appear to regulate

multiple gene clusters in response to simvastatin, including genes for membrane biogenesis (fatty acid biosynthesis), increased drug efflux (ABC and MATE transporters), and heat shock response (DnaK). More work is needed to further characterize how simvastatin interacts with MarR to affect these systems. Dissociation of its genetic target is triggered by ligand binding, which could be due to a direct binding to simvastatin or to another compound that is responsive to simvastatin exposure.

Similarly, our data suggests that the gut bacterium *B. thetaiotaomicron* also uses the cell wall to evade the antibacterial effects of simvastatin. We identified three distinct AcrAB-TolC efflux systems, one of which had been previously characterized as important for the tolerance to the antibacterial fusidic acid which is lipophilic and structurally resembles simvastatin (Liu et al., 2021). These systems are all homologous to *E. coli*, which only encodes a single AcrAB-TolC efflux system (Nikaido & Takatsuka, 2009). More work is needed to assess the substrate-specificity and expression level of *B. thetaiotaomicron*'s different AcrAB-TolC efflux systems and their relative impacts on growth in the presence of simvastatin and other drugs. While all three efflux systems were differentially expressed in the presence of simvastatin, only one of these efflux systems significantly impacted competitive growth in our transposon data, suggesting that system is more important for simvastatin tolerance.

This study has multiple key limitations. The bacterial determinants of susceptibility to simvastatin at the cellular and community level remain to be fully elucidated, but likely involve mechanisms of resistance or other microbe-microbe and host–microbe interactions. Furthermore, it will be important to extend our paired transcriptomic and genetic analyses to additional human gut bacterial species, for example, the simvastatin resistant *Bifidobacterium longum* and *Clostridium sporogenes*, which are both genetically tractable. Of note, prior work has indicated that gut bacteria metabolize simvastatin (Aura et al., 2011; Đanić et al., 2023), which could potentially influence the variation in drug sensitivity we observed. It remains to be explored whether any of the responses observed in this study could be attributed to simvastatin metabolites. While bacterial drug sensitivity was evaluated *in vitro*, more work is needed to assess the susceptibility of gut bacteria to simvastatin *in vivo*, including in gnotobiotic and conventionally raised mice or other model species.

These findings open the door to exploring how simvastatin's antibacterial properties can be contributing to changes in gut microbiome signatures and how they might explain adverse and beneficial effects from statin intake previously observed in metagenomics-based association studies (Vieira-Silva et al., 2020; Zhernakova et al., 2016). Our current results clearly demonstrate the feasibility and utility of focused studies of individual non-antibiotic drugs, like simvastatin, that can have unintended effects for diverse members of the human gut microbiota. Such knowledge sets the foundation for further mechanistic dissection of these drug-microbiome interactions while informing ongoing work in humans looking at cross-sectional and longitudinal differences in the gut microbiome of patients on these widely used medications.

AUTHOR CONTRIBUTIONS

Peter J. Turnbaugh: Conceptualization; funding acquisition; methodology; writing – review and editing; visualization; project administration; resources; supervision. **Veronica Escalante:** Conceptualization; investigation; writing – original draft; methodology; validation; visualization; funding acquisition; data curation. **Renuka R. Nayak:** Methodology; visualization; investigation. **Cecilia Noecker:** Software; visualization; methodology; investigation. **Joel Babdor:** Resources; data curation. **Matthew Spitzer:** Supervision; resources. **Adam M. Deutschbauer:** Resources; supervision.

ACKNOWLEDGMENTS

We thank Moriah Sandy (UCSF Quantitative Metabolite Analysis Center) for analytical support and K.C. Huang (Stanford Department of Bioengineering) for sharing the RB-TnSeq ordered library. National Institutes of Health (R01HL122593, R01AT011117, R01DK114034, R01AR074500, P.J.T.; R25GM056847, V.E.; F32GM140808, C.N.; RM1GM135102, A.M.D.). V.E. received a graduate fellowship from the National Sciences Foundation (1650113). P.J.T. is a Chan Zuckerberg Biohub-San Francisco Investigator (7028823) and held an Investigators in the Pathogenesis of Infectious Disease Award from the Burroughs Wellcome Fund (1017921).

CONFLICT OF INTEREST STATEMENT

The authors declare no competing interests.

DATA AVAILABILITY STATEMENT

Sequencing data are available under NCBI BioProject PRJNA925231.

ETHICS APPROVAL

This study was approved by the University of California San Francisco Institutional Review Board and conducted accordingly. All subjects have given informed consent. This is not a registered clinical trial.

ORCID

Peter J. Turnbaugh https://orcid.org/0000-0002-0888-2875

REFERENCES

Anders, S., Pyl, P.T. & Huber, W. (2014) HTSeq—a python framework to work with high-throughput sequencing data. *Bioinformatics*, 31, 166–169.

Anes, J., McCusker, M.P., Fanning, S. & Martins, M. (2015) The ins and outs of RND efflux pumps in *Escherichia coli*. *Frontiers in Microbiology*, 6, 587. Available from: https://doi.org/10.3389/fmicb.2015.00587

Arjes, H.A., Sun, J., Liu, H., Nguyen, T.H., Culver, R.N., Celis, A.I. et al. (2022) Construction and characterization of a genome-scale ordered mutant collection of *Bacteroides thetaiotaomicron*. *BMC Biology*, 20, 285.

Aura, A.-M., Mattila, I., Hyötyläinen, T., Gopalacharyulu, P., Bounsaythip, C., Orešič, M. et al. (2011) Drug metabolome of the simvastatin formed by human intestinal microbiota *in vitro*. *Molecular BioSystems*, 7, 437–446.

Bisanz, J.E., Soto-Perez, P., Noecker, C., Aksenov, A.A., Lam, K.N., Kenney, G.E. et al. (2020) A genomic toolkit for the mechanistic

dissection of intractable human gut bacteria. *Cell Host & Microbe*, 27, 1001–1013.e9.

Bolyen, E., Rideout, J.R., Dillon, M.R., Bokulich, N.A., Abnet, C.C., Al-Ghalith, G.A. et al. (2019) Reproducible, interactive, scalable and extensible microbiome data science using QIIME 2. *National Biotechnology*, 37, 852–857. Available from: https://doi.org/10.1038/s41587-019-0209-9

Brandvold, K.R., Miller, C.J., Volk, R.F., Killinger, B.J., Whidbey, C. & Wright, A.T. (2021) Activity-based protein profiling of bile salt hydrolysis in the human gut microbiome with beta-lactam or acrylamide-based probes. *Chembiochem*, 22, 1448–1455.

Callahan, B.J., McMurdie, P.J., Rosen, M.J., Han, A.W., Johnson, A.J.A. & Holmes, S.P. (2016) DADA2: high-resolution sample inference from Illumina amplicon data. *Nature Methods*, 13, 581–583.

Caparrós-Martín, J.A., Lareu, R.R., Ramsay, J.P., Peplies, J., Reen, F.J., Headlam, H.A. et al. (2017) Statin therapy causes gut dysbiosis in mice through a PXR-dependent mechanism. *Microbiome*, 5, 95.

Catry, E., Pachikian, B.D., Salazar, N., Neyrinck, A.M., Cani, P.D. & Delzenne, N.M. (2015) Ezetimibe and simvastatin modulate gut microbiota and expression of genes related to cholesterol metabolism. *Life Sciences*, 132, 77–84.

Cheng, T., Li, C., Shen, L., Wang, S., Li, X., Fu, C. et al. (2021) The intestinal effect of atorvastatin: *Akkermansia muciniphila* and barrier function. *Frontiers in Microbiology*, 12, 797062.

Chen, S., Zhou, Y., Chen, Y. & Gu, J. (2018) fastp: an ultra-fast all-in-one FASTQ preprocessor. *Bioinformatics*, 34, i884–i890.

Đanić, M., Pavlović, N., Lazarević, S., Stanimirov, B., Vukmirović, S., Al-Salami, H. et al. (2023) Bioaccumulation and biotransformation of simvastatin in probiotic bacteria: a step towards better understanding of drug-bile acids-microbiome interactions. *Frontiers in Pharmacology*, 14, 1111115.

Davlieva, M., Zhang, W., Arias, C.A. & Shamoo, Y. (2013) Biochemical characterization of cardiolipin synthase mutations associated with daptomycin resistance in enterococci. *Antimicrobial Agents and Chemotherapy*, 57, 289–296.

DeSantis, T.Z., Hugenholtz, P., Larsen, N., Rojas, M., Brodie, E.L., Keller, K. et al. (2006) Greengenes, a chimera-checked 16S rRNA gene database and workbench compatible with ARB. *Applied and Environmental Microbiology*, 72, 5069–5072.

Dixon, P. (2003) VEGAN, a package of R functions for community ecology. *Journal of Vegetation Science*, 14, 927–930. Available from: https://doi.org/10.1111/j.1654-1103.2003.tb02228.x

Edgar, R.C. (2004) MUSCLE: multiple sequence alignment with high accuracy and high throughput. *Nucleic Acids Research*, 32, 1792–1797.

Falony, G., Joossens, M., Vieira-Silva, S., Wang, J., Darzi, Y., Faust, K. et al. (2016) Population-level analysis of gut microbiome variation. *Science*, 352, 560–564.

Fernandes, A.D., Macklaim, J.M., Linn, T.G., Reid, G. & Gloor, G.B. (2013) ANOVA-like differential expression (ALDEx) analysis for mixed population RNA-Seq. *PLoS One*, 8, e67019.

Fernandes, A.D., Reid, J.N., Macklaim, J.M., McMurrough, T.A., Edgell, D.R. & Gloor, G.B. (2014) Unifying the analysis of high-throughput sequencing datasets: characterizing RNA-seq, 16S rRNA gene sequencing and selective growth experiments by compositional data analysis. *Microbiome*, 2, 15.

Gill, S.R., Pop, M., Deboy, R.T., Eckburg, P.B., Turnbaugh, P.J., Samuel, B.S. et al. (2006) Metagenomic analysis of the human distal gut microbiome. *Science*, 312, 1355–1359.

Gohl, D.M., Vangay, P., Garbe, J., MacLean, A., Hauge, A., Becker, A. et al. (2016) Systematic improvement of amplicon marker gene methods for increased accuracy in microbiome studies. *Nature Biotechnology*, 34, 942–949.

Golomb, B.A. & Evans, M.A. (2008) Statin adverse effects: a review of the literature and evidence for a mitochondrial mechanism. *American Journal of Cardiovascular Drugs*, 8, 373–418.

Grove, A. (2013) MarR family transcription factors. *Current Biology*, 23, R142–R143.

Guindon, S., Dufayard, J.-F., Lefort, V., Anisimova, M., Hordijk, W. & Gascuel, O. (2010) New algorithms and methods to estimate maximum-likelihood phylogenies: assessing the performance of PhyML 3.0. *Systematic Biology*, 59, 307–321.

Gurbich, T.A., Almeida, A., Beracochea, M., Burdett, T., Burgin, J., Cochrane, G. et al. (2023) MGnify Genomes: a resource for biome-specific microbial genome catalogues. *Journal of Molecular Biology*, 435, 168016.

Heuston, S., Begley, M., Gahan, C.G.M. & Hill, C. (2012) Isoprenoid biosynthesis in bacterial pathogens. *Microbiology*, 158, 1389–1401.

He, X., Zheng, N., He, J., Liu, C., Feng, J., Jia, W. et al. (2017) Gut microbiota modulation attenuated the Hypolipidemic effect of simvastatin in high-fat/cholesterol-diet fed mice. *Journal of Proteome Research*, 16, 1900–1910.

Huang, Y.Y., Price, M.N., Hung, A., Gal-Oz, O., Ho, D., Carion, H., et al. (2022) Functional screens of barcoded expression libraries uncover new gene functions in carbon utilization among gut Bacteroidales. *bioRxiv* 2022.10.10.511384. Available from: https://doi.org/10.1101/2022.10.10.511384. [Accessed 7th February 2023].

Huerta-Cepas, J., Szklarczyk, D., Heller, D., Hernández-Plaza, A., Forslund, S.K., Cook, H. et al. (2019) eggNOG 5.0: a hierarchical, functionally and phylogenetically annotated orthology resource based on 5090 organisms and 2502 viruses. *Nucleic Acids Research*, 47(D1), D309–D314. Available from: https://doi.org/10.1093/nar/gky1085

Kaddurah-Daouk, R., Baillie, R.A., Zhu, H., Zeng, Z.-B., Wiest, M.M., Nguyen, U.T. et al. (2011) Enteric microbiome metabolites correlate with response to simvastatin treatment. *PLoS One*, 6, e25482.

Kanehisa, M., Sato, Y. & Morishima, K. (2016) BlastKOALA and GhostKOALA: KEGG tools for functional characterization of genome and metagenome sequences. *Journal of Molecular Biology*, 428, 726–731.

Ko, H.H.T., Lareu, R.R., Dix, B.R. & Hughes, J.D. (2017) Statins: antimicrobial resistance breakers or makers? *PeerJ*, 5, e3952.

Lamers, R.P., Cavallari, J.F. & Burrows, L.L. (2013) The efflux inhibitor phenylalanine-arginine beta-naphthylamide (PAβN) permeabilizes the outer membrane of gram-negative bacteria. *PLoS One*, 8, e60666.

Langmead, B. & Salzberg, S.L. (2012) Fast gapped-read alignment with Bowtie 2. *Nature Methods*, 9, 357–359.

Lechner, M., Findeiss, S., Steiner, L., Marz, M., Stadler, P.F. & Prohaska, S.J. (2011) Proteinortho: detection of (co-)orthologs in large-scale analysis. *BMC Bioinformatics*, 12, 124.

Liu, H., Shiver, A.L., Price, M.N., Carlson, H.K., Trotter, V.V., Chen, Y. et al. (2021) Functional genetics of human gut commensal *Bacteroides thetaiotaomicron* reveals metabolic requirements for growth across environments. *Cell Reports*, 34, 108789.

Li, X.-Z. & Nikaido, H. (2009) Efflux-mediated drug resistance in bacteria: an update. *Drugs*, 69, 1555–1623.

Lomovskaya, O., Lewis, K. & Matin, A. (1995) EmrR is a negative regulator of the *Escherichia coli* multidrug resistance pump EmrAB. *Journal of Bacteriology*, 177, 2328–2334.

Love, M.I., Huber, W. & Anders, S. (2014) Moderated estimation of fold change and dispersion for RNA-seq data with DESeq2. *Genome Biology*, 15, 550.

Maier, L., Pruteanu, M., Kuhn, M., Zeller, G., Telzerow, A., Anderson, E.E. et al. (2018) Extensive impact of non-antibiotic drugs on human gut bacteria. *Nature*, 555, 623–628.

Maurice, C.F., Haiser, H.J. & Turnbaugh, P.J. (2013) Xenobiotics shape the physiology and gene expression of the active human gut microbiome. *Cell*, 152, 39–50.

McMurdie, P.J. & Holmes, S. (2013) Phyloseq: an R package for reproducible interactive analysis and graphics of microbiome census data. *PLoS One*, 8, e61217.

Nayak, R.R., Alexander, M., Deshpande, I., Stapleton-Gray, K., Rimal, B., Patterson, A.D. et al. (2021) Methotrexate impacts conserved pathways in diverse human gut bacteria leading to decreased host immune activation. *Cell Host & Microbe*, 29, 362–377.e11. Available from: https://doi.org/10.1016/j.chom.2020.12.008

Nikaido, H. & Takatsuka, Y. (2009) Mechanisms of RND multidrug efflux pumps. *Biochimica et Biophysica Acta*, 1794, 769–781.

Okonechnikov, K., Golosova, O., Fursov, M. & UGENE team. (2012) Unipro UGENE: a unified bioinformatics toolkit. *Bioinformatics*, 28, 1166–1167.

Paradis, E., Claude, J. & Strimmer, K. (2004) APE: analyses of Phylogenetics and evolution in R language. *Bioinformatics*, 20, 289–290.

Perera, I.C. & Grove, A. (2010) Molecular mechanisms of ligand-mediated attenuation of DNA binding by MarR family transcriptional regulators. *Journal of Molecular Cell Biology*, 2, 243–254.

Poole, K., Tetro, K., Zhao, Q., Neshat, S., Heinrichs, D.E. & Bianco, N. (1996) Expression of the multidrug resistance operon mexA-mexB-oprM in *Pseudomonas aeruginosa*: mexR encodes a regulator of operon expression. *Antimicrobial Agents and Chemotherapy*, 40, 2021–2028.

Price, M.N., Wetmore, K.M., Waters, R.J., Callaghan, M., Ray, J., Liu, H. et al. (2018) Mutant phenotypes for thousands of bacterial genes of unknown function. *Nature*, 557, 503–509.

Royce, L.A., Liu, P., Stebbins, M.J., Hanson, B.C. & Jarboe, L.R. (2013) The damaging effects of short chain fatty acids on *Escherichia coli* membranes. *Applied Microbiology and Biotechnology*, 97, 8317–8327.

Sinha, R., Stanley, G., Gulati, G.S., Ezran, C., Travaglini, K.J., Wei, E., et al. (2017) Index switching causes "spreading-of-signal" among multiplexed samples in Illumina HiSeq 4000 DNA sequencing. *bioRxiv* 125724. Available from: https://doi.org/10.1101/125724. [Accessed 6th September 2022].

Spanogiannopoulos, P., Kyaw, T.S., Guthrie, B.G.H., Bradley, P.H., Lee, J.V., Melamed, J. et al. (2022) Host and gut bacteria share metabolic pathways for anti-cancer drug metabolism. *Nature Microbiology*, 7, 1605–1620. Available from: https://doi.org/10.1038/s41564-022-01226-5

Sprouffske, K. & Wagner, A. (2016) Growthcurver: an R package for obtaining interpretable metrics from microbial growth curves. *BMC Bioinformatics*, 17, 172.

Srikumar, R., Paul, C.J. & Poole, K. (2000) Influence of mutations in the mexR repressor gene on expression of the MexA-MexB-oprM multidrug efflux system of Pseudomonas aeruginosa. *Journal of Bacteriology*, 182, 1410–1414.

Sulavik, M.C., Gambino, L.F. & Miller, P.F. (1995) The MarR repressor of the multiple antibiotic resistance (mar) operon in *Escherichia coli*: prototypic member of a family of bacterial regulatory proteins involved in sensing phenolic compounds. *Molecular Medicine*, 1, 436–446.

Su, Y.-B., Kuang, S.-F., Ye, J.-Z., Tao, J.-J., Li, H., Peng, X.-X. et al. (2021) Enhanced biosynthesis of fatty acids is associated with the acquisition of ciprofloxacin resistance in *Edwardsiella tarda*. *mSystems*, 6, e0069421.

Vieira-Silva, S., Falony, G., Belda, E., Nielsen, T., Aron-Wisnewsky, J., Chakaroun, R. et al. (2020) Statin therapy is associated with lower prevalence of gut microbiota dysbiosis. *Nature*, 581, 310–315.

Wang, Q., Garrity, G.M., Tiedje, J.M. & Cole, J.R. (2007) Naive Bayesian classifier for rapid assignment of rRNA sequences into the new bacterial taxonomy. *Applied and Environmental Microbiology*, 73, 5261–5267.

Wetmore, K.M., Price, M.N., Waters, R.J., Lamson, J.S., He, J., Hoover, C.A. et al. (2015) Rapid quantification of mutant fitness in diverse bacteria by sequencing randomly bar-coded transposons. *mBio*, 6, e00306-15.

Wickham, H. (2016) Data Analysis. In: Wickham, H. (Ed.) *ggplot2: elegant graphics for data analysis*. Cham: Springer International Publishing, pp. 189–201.

Wilmanski, T., Kornilov, S.A., Diener, C., Conomos, M.P., Lovejoy, J.C., Sebastiani, P. et al. (2022) Heterogeneity in statin responses explained by variation in the human gut microbiome. *Med (N Y)*, 3, 388–405.e6.

Wishart, D.S., Feunang, Y.D., Guo, A.C., Lo, E.J., Marcu, A., Grant, J.R. et al. (2018) DrugBank 5.0: a major update to the DrugBank database for 2018. *Nucleic Acids Research*, 46, D1074–D1082.

Xiong, A., Gottman, A., Park, C., Baetens, M., Pandza, S. & Matin, A. (2000) The EmrR protein represses the *Escherichia coli* emrRAB multidrug resistance operon by directly binding to its promoter region. *Antimicrobial Agents and Chemotherapy*, 44, 2905–2907.

Xu, M., Luo, L.-L., Du, M.-Y., Tang, L., Zhou, J., Hu, Y. et al. (2022) Simvastatin improves outcomes of endotoxin-induced coagulopathy by regulating intestinal microenvironment. *Current Medical Science*, 42, 26–38.

Yu, G., Lam, T.T.-Y., Zhu, H. & Guan, Y. (2018) Two methods for mapping and visualizing associated data on phylogeny using Ggtree. *Molecular Biology and Evolution*, 35, 3041–3043.

Yu, G., Wang, L.-G., Han, Y. & He, Q.-Y. (2012) clusterProfiler: an R package for comparing biological themes among gene clusters. *Omics*, 16, 284–287.

Zdobnov, E.M. & Apweiler, R. (2001) InterProScan—an integration platform for the signature-recognition methods in InterPro. *Bioinformatics*, 17, 847–848.

Zhang, P., Zhang, X., Huang, Y., Chen, J., Shang, W., Shi, G. et al. (2021) Atorvastatin alleviates microglia-mediated neuroinflammation via modulating the microbial composition and the intestinal barrier function in ischemic stroke mice. *Free Radical Biology & Medicine*, 162, 104–117.

Zhernakova, A., Kurilshikov, A., Bonder, M.J., Tigchelaar, E.F., Schirmer, M., Vatanen, T. et al. (2016) Population-based metagenomics analysis reveals markers for gut microbiome composition and diversity. *Science*, 352, 565–569.

Zou, L., Spanogiannopoulos, P., Pieper, L.M., Chien, H.-C., Cai, W., Khuri, N. et al. (2020) Bacterial metabolism rescues the inhibition of intestinal drug absorption by food and drug additives. *Proceedings of the National Academy of Sciences of the United States of America*, 117, 16009–16018.

SUPPORTING INFORMATION

Additional supporting information can be found online in the Supporting Information section at the end of this article.

How to cite this article: Escalante, V., Nayak, R.R., Noecker, C., Babdor, J., Spitzer, M., Deutschbauer, A.M. et al. (2023) Simvastatin induces human gut bacterial cell surface genes. *Molecular Microbiology*, 00, 1–15. Available from: https://doi.org/10.1111/mmi.15151